

First-Principles Study of the Structural, Electronic, Magnetic, Elastic, and Optical Properties of CoFeZrSi Quaternary Heusler Alloy

Yasser Ahmed Behlali 1, Abdelaziz Amara 2, Salima Labidi 2, Seifeddine Amara 1 2 3

1 LEAM Laboratory, Department of Physics, Faculty of Sciences, Badji Mokhtar – Annaba University, Po. Box 12, Annaba 23000, Algeria  
2 Laboratory of LEREC, Department of Physics, Faculty of Sciences, Badji Mokhtar – Annaba University, Po. Box 12, Annaba 23000, Algeria. E-mail: [abdelaziz.amara@univ-annaba.dz](mailto:abdelaziz.amara@univ-annaba.dz)  
3 LNCTS Laboratory, Department of Physics, Faculty of Sciences, Badji Mokhtar – Annaba University, Po. Box 12, Annaba 23000, Algeria

INTRODUCTION AND AIM

Quaternary Heusler alloys (QHAs) have recently emerged as a fascinating class of intermetallic compounds because of their wide range of tunable properties and potential applications. These alloys, with a general formula  $XXYZ$ , combine three transition metals and one main group element in a highly symmetric cubic structure, offering a flexible platform to design new materials with tailored functionalities. One of the most attractive features of QHAs is their tendency to exhibit half-metallic ferromagnetism, where electrons of one spin channel behave metallic while those of the opposite spin channel show semiconducting character. This unique property leads to 100% spin polarization at the Fermi level, making them highly promising for next-generation spintronic devices such as magnetic sensors, memory storage, and spin filters [1]. Beyond their magnetic features, QHAs have also been investigated for their mechanical stability and elastic behavior, which are crucial for practical device integration. Furthermore, their optical absorption, dielectric response, and plasmonic characteristics suggest promising roles in optoelectronic and photonic technologies. The ability to combine strong magnetic ordering, mechanical robustness, and efficient light–matter interaction within a single material family makes these alloys particularly valuable for multifunctional applications. In this work, we present a comprehensive study of the CoFeZrSi quaternary Heusler alloy based on first-principles DFT calculations. We systematically examine its structural stability, electronic band structure, magnetic moments, elastic constants, and optical properties. The aim is to understand the fundamental physical behavior of CoFeZrSi and assess its potential for applications in advanced spintronics, optoelectronics, and energy-related technologies.

METHOD

The first-principles calculations were performed within the framework of density functional theory (DFT) using the full-potential linearized augmented plane wave (FP-LAPW) method implemented in the WIEN2k code [2]. The generalized gradient approximation (GGA) [3] was employed to describe the exchange–correlation energy, while the modified Becke–Johnson (mBJ) [4] potential was applied to improve the accuracy of electronic and optical property predictions. A cutoff parameter of  $RMT_{Kmax} = 8$  and a Monkhorst–Pack grid of 3000 k-points were used for Brillouin zone sampling. The separation of valence and core states was set at  $-6.0$  Ry, and convergence of the self-consistent cycles was achieved at  $0.0001e$ . In addition, the elastic constants were calculated using the IRelast package [5] to ensure the mechanical stability of the compound.

RESULTS & DISCUSSION

Structural properties:

The quaternary Heusler alloy (QHA) CoFeZrSi crystallizes in the cubic LiMgPdSb-type structure, known as the Y-type, with space group  $F43m_{-}43m$ . This structure has a stoichiometric composition of  $XX'YZ$ , where X, X', and Y are transition metals and Z is an s- or p-block element, and it can exist in three nonequivalent configurations (Y1, Y2, and Y3), whose Wyckoff positions are summarized in Table 1. To identify the most stable atomic arrangement, we performed structural optimizations by calculating the total energy as a function of volume for the three configurations under both non-spin-polarized and spin-polarized conditions. The results, displayed in Fig. 1, clearly indicate that the ferromagnetic Y1 structure exhibits the lowest total energy, confirming it as the most stable phase for CoFeZrSi. The optimized lattice parameters and other calculated structural constants for this configuration are provided in Table 2.

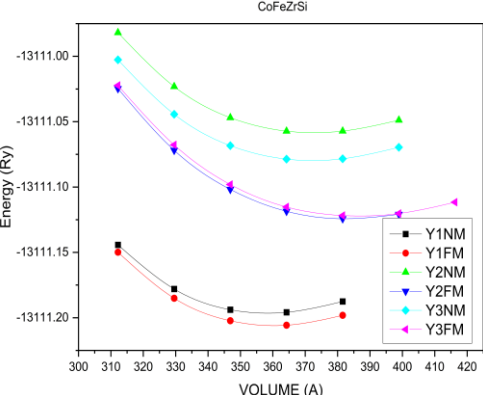


Fig. 1: Energy variation as a function of volume.

Table 1: Wyckoff position of Y1, Y2, and Y3 configurations.

	X	X'	Y	Z
Y1	3/4	1/4	1/2	0
Y2	3/4	1/2	1/4	0
Y3	3/4	0	1/2	1/4

Table 2: Optimized structural properties, lattice constants (a), bulk modulus (B), derivative pressure (B'), total energy (Emin).

Type	a(Å)	B(GPa)	B'	E <sub>min</sub> (Ry)
Y1	5.9771	202.3246	4.0584	-13111.20
Y2	6.1128	158.2392	3.1326	-13111.12
Y3	6.1179	151.6508	3.4509	-13111.12
Y1NM	5.9673	198.8137	4.5843	-13111.19

Electronic and magnetic properties:

The electronic and magnetic properties of CoFeZrSi were investigated using first-principles calculations within the PBE-GGA and TB-mBJ approximations. The spin-polarized band structures (Figs. 2–3) reveal metallic behavior in the spin-up channel, where the valence band overlaps with the Fermi level, while the spin-down channel exhibits an indirect  $\Gamma$ –X band gap of 0.66 eV within PBE-GGA and 1.45 eV with TB-mBJ. This confirms the half-metallic nature of CoFeZrSi, with the gap value being significantly enhanced under the mBJ correction. The total and partial densities of states (Fig. 4) further support this behavior, showing that the Fermi level falls within the minority spin gap, whereas the majority spin states cross the Fermi level. In the energy range  $-4$  to  $2$  eV, the DOS is dominated by strong hybridization between Co and Fe d-states, while Zr d-states contribute mainly in the  $2$ – $4$  eV region; the s,p states of Si remain far from the Fermi level and play a limited role in gap formation. Magnetic moment calculations (Table 3) indicate that CoFeZrSi carries an integer total moment of  $1 \mu_B$ , in good agreement with the Slater–Pauling rule  $M_{Tot} = Z_{tot} - 24$  [6]. The main contributions arise from Co and Fe atoms, while Zr and Si provide negligible values. Moreover, the computed spin polarization at the Fermi level reaches 100%, confirming that CoFeZrSi is a half-metallic ferromagnet with full spin polarization, a property that makes it a strong candidate for spintronic applications.

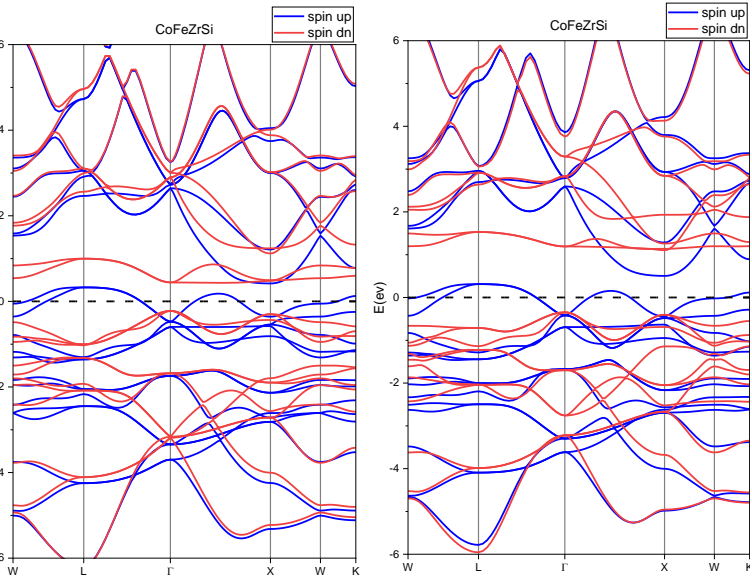


Fig. 2: Band structure using PBE-GGA method

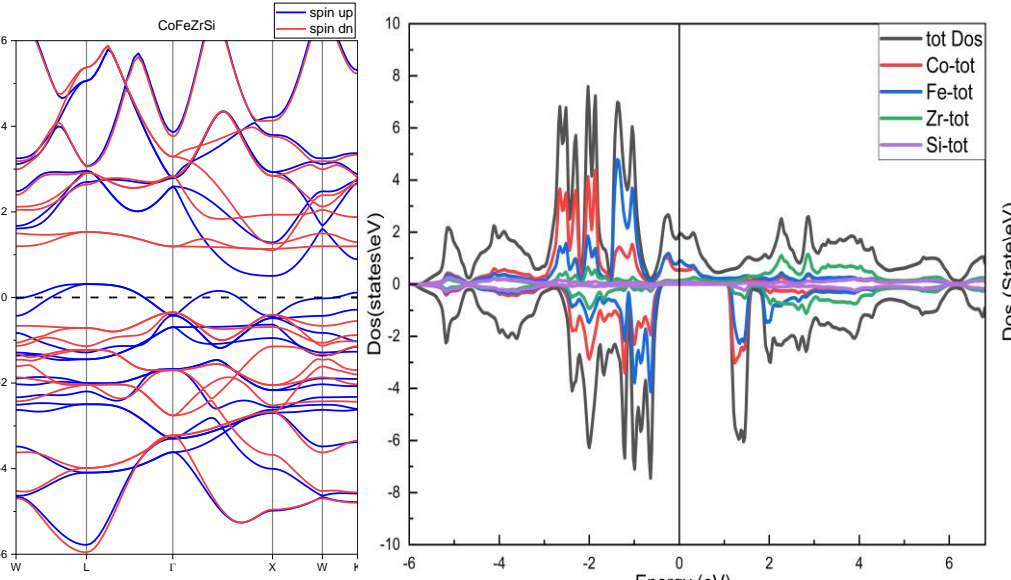


Fig. 3: Band structure using mBJ-GGA method

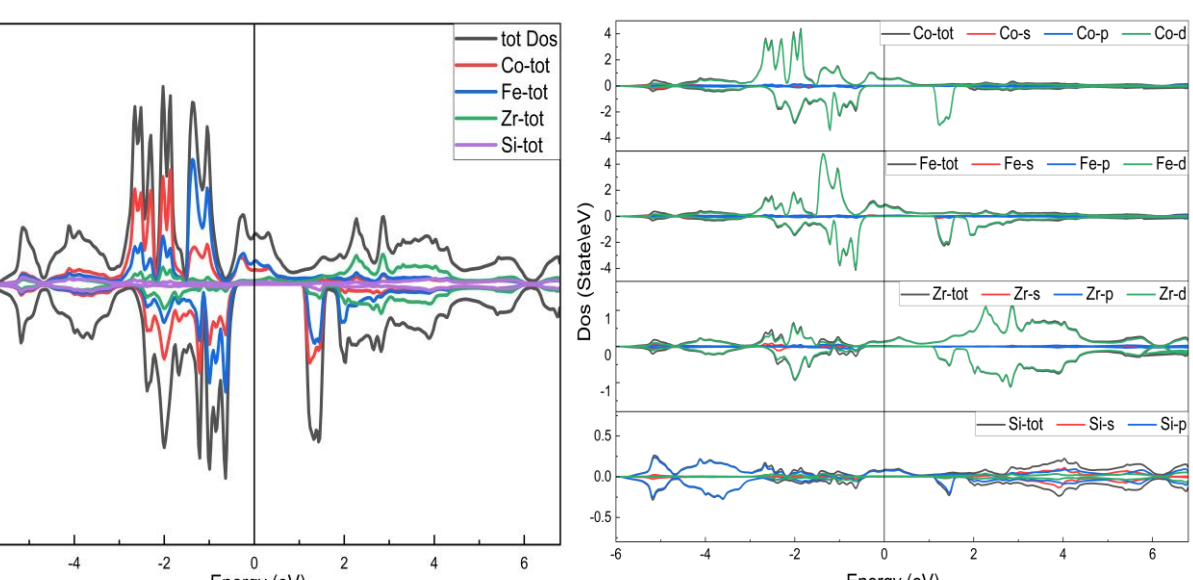


Fig. 4: Total and partial densities of states (TDOS and PDOS) for CoFeZrSi in his stable structure using mBJ-GGA method..

Table 3: The computed total, interstitial, partial magnetic moment, and spin polarization for CoFeZrSi alloy.

	$\mu^{Total}(\mu_B/Cell)$ Slater-Pauling rule	$\mu^{interstitial}(\mu_B/Cell)$	$\mu_{Co}$	$\mu_{Fe}$	$\mu_{Zr}$	$\mu_{Si}$	P (%)	E <sub>g</sub>
PBE-GGA	1.00	-0.11	0.57	0.66	-0.08	-0.0002	100%	0.66
mBJ-GGA	1.00	-0.24	0.71	0.69	-0.15	-0.018	100%	1.45

Elastic Properties:

The independent elastic constants of CoFeZrSi, presented in Table 4, satisfy the Born–Huang stability conditions for cubic systems:  $(C_{11} - C_{12}) > 0$ ,  $C_{11} > 0$ ,  $C_{44} > 0$ ,  $(C_{11} + 2C_{12}) > 0$ , thus, confirming the mechanical stability of the alloy at 0K. The relatively large  $C_{11}$  compared to  $C_{44}$  indicates that CoFeZrSi resists axial compression more strongly than shear deformation. This trend is consistent with the bulk modulus ( $B = 189.12$  GPa) exceeding the shear modulus ( $G = 52.95$  GPa), which also reflects metallic bonding. The corresponding Young's modulus ( $E = 145.30$  GPa) indicates moderate stiffness of the alloy. Ductility was evaluated through Pugh's ratio ( $B/G = 3.57$ ), Poisson's ratio ( $\nu = 0.37$ ), and Cauchy pressure ( $C_{12} - C_{44} = 100.77$  GPa). All values confirm the ductile metallic character of CoFeZrSi. The relatively low Vickers hardness ( $H_V = 4.52$  GPa) supports this conclusion, while the machinability index ( $\mu_m = 3.44$ ) suggests that the alloy is easily workable, which is beneficial for processing in device fabrication. Thermal and isotropic behavior is described in Table 5. The universal anisotropy index ( $A_u = 0.01$ ) is nearly zero, demonstrating that CoFeZrSi is elastically isotropic, ensuring uniform mechanical response along different crystallographic directions. Furthermore, the calculated Debye temperature ( $\Theta_D \approx 440$  K) and melting point ( $T_m \approx 2066$  K) confirm the alloy's thermal stability. In summary, the results in Table 4 and 5 reveal that CoFeZrSi is a mechanically stable, ductile, isotropic, and thermally robust quaternary Heusler alloy, which makes it a promising candidate for future technological applications.

Table 4: Calculated elastic constants Cij, Bulk modulus B (GPa), shear modulus G (GPa), Young's modulus E (GPa), Poisson's ratio  $\nu$ , Cauchy's pressure Cp (GPa), and B/G, Vickers hardness H, machinability index  $\mu_m$ , Kleinman parameter  $\zeta$  ratio.

Compound	$C_{11}$ (GPa)	$C_{12}$ (GPa)	$C_{44}$ (GPa)	B (GPa)	G (GPa)	E (GPa)	$\nu$	$C_{12}-C_{44}$ (GPa)	B/G	H (GPa)	$\mu_m$	$\zeta$
CoFeZrSi	255.98	155.69	54.91	189.12	52.95	145.30	0.37	100.77	3.57	4.52	3.44	0.71

Table 5: Computed  $\rho$  (Kg/m3),  $V_t$ (m/s),  $V_l$ (m/s),  $V_m$ (m/s), Universal (Au) and Zener (Az) anisotropy, Lamé's constants ( $\lambda$ ,  $\mu$ ), Grüneisen parameter  $\zeta_{ac}$  melting  $T_m$ (K) and Debye temperature  $\Theta_D$  (K).

Compound	$\rho$ (Kg/m <sup>3</sup> )	m (g/mol)	$V_t$ (m/s)	$V_l$ (m/s)	$V_m$ (m/s)	A <sup>u</sup>	A <sup>z</sup>	$\mu$	$\lambda$	$\zeta^{ac}$	T <sub>m</sub> (k)	$\Theta_D$ (k)	
CoFeZrSi												$\Theta_D^{Heusler}$	$\Theta_D^{ac}$
	7281	234.08	2696	6122	3044	0,01	1,09	52,9	153,8	2,40	2066	440	382

Optical properties:

The optical properties of CoFeZrSi were investigated using the modified Beck–Johnson potential (mBJ) within the generalized gradient approximation (GGA) in the photon energy range of  $0$ – $35$  eV. The real part of the dielectric function  $\epsilon_1(\omega)$  shows negative values at low energies, reflecting metallic characteristics, and becomes positive at higher energies, while the imaginary part  $\epsilon_2(\omega)$  exhibits pronounced peaks associated with interband transitions. The refractive index reaches its maximum in the low-energy region and decreases gradually with increasing photon energy, whereas the extinction coefficient increases significantly in the visible–UV domain, indicating strong absorption. Reflectivity remains high at low energies but drops with energy, consistent with metallic screening, while the optical conductivity reveals distinct peaks originating from electronic transitions. The absorption coefficient attains values on the order of  $10^5 \text{ cm}^{-1}$ , confirming efficient photon absorption, and the energy loss function displays plasmon peaks corresponding to collective electron oscillations. Overall, these results demonstrate that CoFeZrSi possesses strong interband absorption and plasmonic features, suggesting its suitability for optoelectronic and photonic applications.

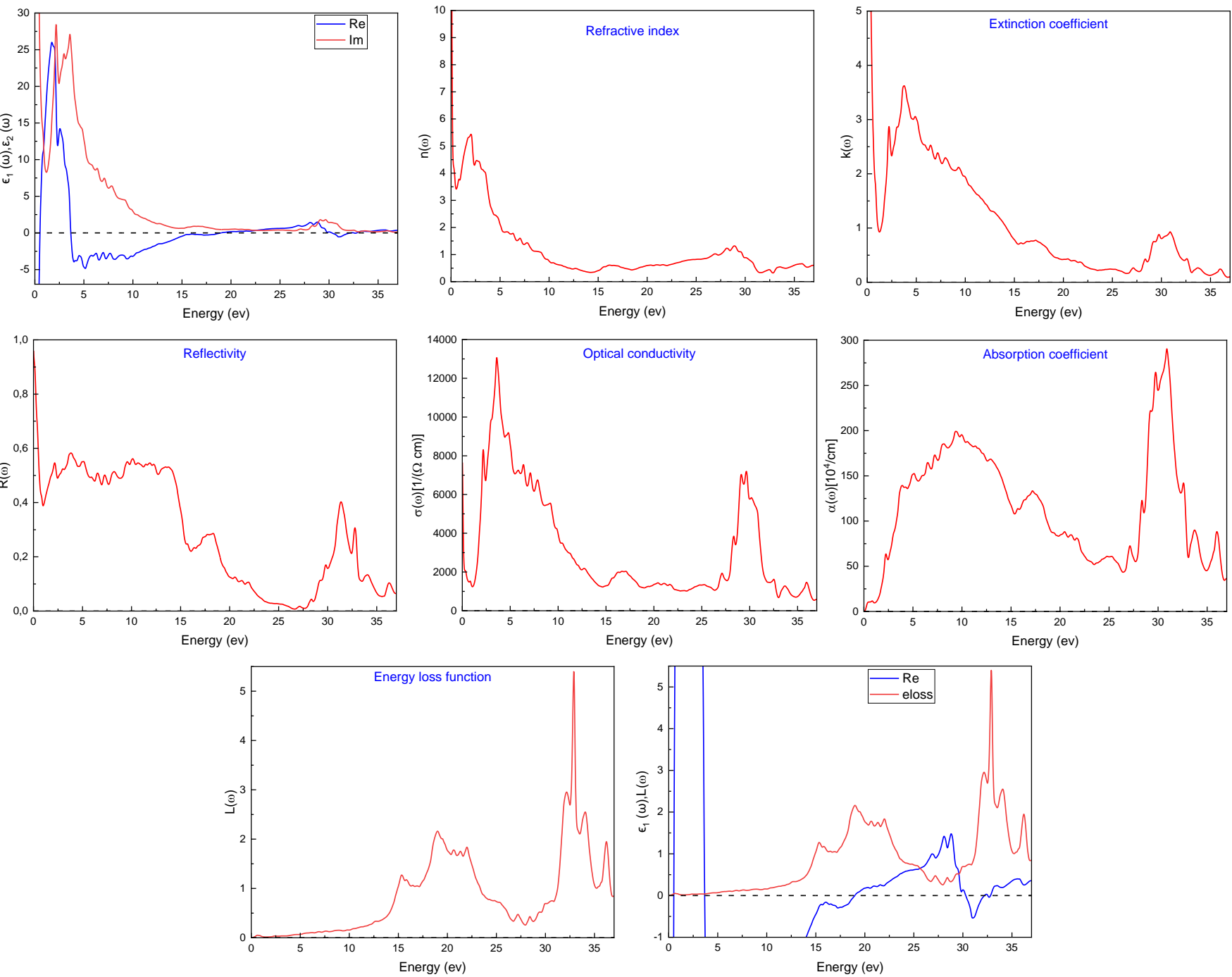


Fig. 6: Refractive index  $n(\omega)$ , extinction coefficient  $K(\omega)$ , reflectivity  $R(\omega)$ , optical conductivity  $\sigma(\omega)$ , absorption coefficient  $\alpha(\omega)$ , and energy loss function  $L(\omega)$  for CoFeZrSi under modified Beck–Johnson potential (mBJ)-generalized gradient approximation (GGA) approximation.

CONCLUSION

First-principles calculations confirmed that CoFeZrSi crystallizes in the stable cubic Y1-type structure with ferromagnetic ordering. The electronic and magnetic analyses revealed a half-metallic ferromagnetic character with 100% spin polarization at the Fermi level and an integer magnetic moment consistent with the Slater–Pauling rule, highlighting its potential for spintronic applications. The elastic constants (Table 4) fulfill the Born–Huang criteria, demonstrating mechanical stability, ductility, excellent machinability, and near isotropy, together with good thermal stability. Furthermore, the optical investigation showed strong absorption, high reflectivity in the infrared, and pronounced plasmonic peaks, confirming suitability for optoelectronic and photonic devices. Overall, the combination of mechanical robustness, half-metallic ferromagnetism, and promising optical behavior makes CoFeZrSi a versatile quaternary Heusler alloy with significant potential for advanced spintronic, optoelectronic, and energy-related technologies.

REFERENCES

[1] Şaşgölu E, Blügel S, Mertig I. Proposal for reconfigurable magnetic tunnel diode and transistor. ACS Appl Electron Mater. 2019;1(8):1552–59. <https://doi.org/10.1021/ACSAELM.9B00318>  
[2] Schwarz K, Blaha P. Solid state calculations using WIEN2k. Comput Mater Sci. 2003;28(2):259–73. [https://doi.org/10.1016/S0927-0256\(03\)00112-5](https://doi.org/10.1016/S0927-0256(03)00112-5)  
[3] Perdew JP, Burke K, Ernzerhof M. Generalized gradient approximation made simple. Phys Rev Lett. 1996;77(18):3865 68. <https://doi.org/10.1103/PhysRevLett.77.3865>  
[4] Koller D, Tran F, Blaha P. Improving the modified Becke–Johnson exchange potential. Phys Rev B—Condens Matter Mater Phys. 2012;85(15):155109. <https://doi.org/10.1103/PhysRevB.85.155109>  
[5] Jamal M, Bilal M, Ahmad I, Jalali-Asadabadi S. IRelast package. J Alloys Compd. 2018;735:569–79. <https://doi.org/10.1016/J.JALLCOM.2017.10.139>  
[6] Galanakis I, Dederichs PH, Papanikolaou N. Slater–Pauling behavior and origin of the half-metallicity of the full-Heusler alloys. Phys Rev B. 2002;66(17):174429. <https://doi.org/10.1103/PhysRevB.66.174429>